

# Rechargeable Seawater Battery and Its Electrochemical Mechanism

Jae-Kwang Kim<sup>1†</sup>, Eungje Lee<sup>2†</sup>, Hyojin Kim<sup>1</sup>, Christopher Johnson<sup>2</sup>, Jaephil Cho<sup>1,\*</sup> and  
Youngsik Kim<sup>1,\*</sup>

<sup>1</sup> Interdisciplinary School of Green Energy, Ulsan National Institute of Science and Technology (UNIST), Ulsan 689-798, Korea

<sup>2</sup> Chemical Science and Engineering Division, Argonne National Laboratory, Argonne, IL 60439, USA

<sup>3</sup> Richard Lugar Center for Renewable Energy, Indiana University Purdue University Indianapolis (IUPUI), Indianapolis, IN 46202, USA

† J.K.K. and E.L. contribute equally to this work.

\* Corresponding authors: J. Cho ([jpcho@unist.ac.kr](mailto:jpcho@unist.ac.kr)) and Y. Kim ([ykim@unist.ac.kr](mailto:ykim@unist.ac.kr))

**Herein, we explore the electrochemical mechanism of a novel rechargeable seawater battery system that uses seawater as the cathode material. Sodium is harvested from seawater while charging the battery, and the harvested sodium is discharged with oxygen dissolved in the seawater, functioning as oxidants to produce electricity. The seawater provides both anode (Na metal) and cathode (O<sub>2</sub>) materials for the proposed battery. Based on the discharge voltage (~2.9 V) with participation of O<sub>2</sub> and the charge voltage (~4.1 V) with Cl<sub>2</sub> evolution during the first cycle, a voltage efficiency of about 73% is obtained. If the seawater battery is constructed using hard carbon as the anode and a Na super ion conductor as the solid electrolyte, a strong cycle performance of 84% is observed after 40 cycles.**

The requirements for energy-storage systems are vastly different from those for consumer electronics or electric vehicles (EVs) and vary widely depending on factors such as installation size and location. This makes it difficult for one type of battery systems to become a predominant solution satisfying all the requirements. Instead, a reasonable and practical strategy is to respond to diverse requirements of each application with various alternative battery systems considering the characteristics of each option. For example, while an advanced Li-ion battery, which has a high volumetric energy density, would be a right choice for the energy storage in densely populated areas considering its high volumetric energy density, other bulky but cheaper systems could become more competitive in remote areas where the size of systems can be easily expanded. Therefore, it is important to build a strong portfolio of novel battery systems to provide optimum solutions.

The development of novel configurations of battery cells, such as Li–Air,[1] Li–liquid,[2] Na–air,[3] and Li–polysulfide batteries,[4] has been made possible by combinations

of multi-phase electrolyte/electrode components such as liquid/solid electrolytes and liquid/solid/liquid (or gas) electrodes. Based on these battery designs, various interesting combinations of electrochemical reaction couples are being suggested and tested that were not previously considered due to the limitations of conventional battery cell design.

Recently, we investigated the feasibility of a novel rechargeable battery system using seawater as an electrode material.[5] As the most abundant resource on Earth, seawater contains various chemical species released from the Earth's crust and living organisms. Examples of the major chemical constituents of seawater are sodium (Na) (~0.46 M) and chlorides (~0.54 M).[6] Detailed information on the chemical constituents of seawater is shown in Figure 1a. Accordingly, we constructed a novel rechargeable battery cell that uses seawater and its chemical constituents as anode/cathode materials. The configuration of the seawater battery, composed of Na/non-aqueous liquid/solid electrolyte/seawater, is shown in Figure 1b and Figure 1c. 1 M NaClO<sub>4</sub> in ethylene carbonate: diethyl carbonate (1:1 volume ratio) was used as the non-aqueous liquid electrolyte. Direct contact between the flowing seawater at the positive electrode and the liquid electrolyte in the negative electrode compartment was prevented by the NASICON-type (NASICON:Na super ion conductor) Na<sub>3</sub>Zr<sub>2</sub>Si<sub>2</sub>PO<sub>12</sub> solid electrolyte, which has a good crystallinity (see Figure S1 in the Supporting Information, SI) and a rapid Na ion conductivity of  $>7.0 \times 10^{-4} \text{ S cm}^{-1}$  at room temperature (Figure S2). Following the above innovative cell concept, the mechanism of the seawater battery is demonstrated in this work.

Sodium ion transport and the potential chemical reaction mechanisms in the cell during the charge and discharge processes are shown as schematic diagrams in Figures 1b and 1c, respectively. The charge curve of the prepared seawater battery is shown in Figure 2a.

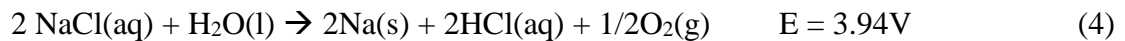
Salt water [0.1 M NaCl (aq)] was also tested under the same experimental conditions, and a charge voltage of ~4.1 V (vs. Na<sup>+</sup>/Na<sup>0</sup>) was obtained and compared to that of the seawater (~4.0 V vs. Na<sup>+</sup>/Na<sup>0</sup>), as shown in Figure 2 a. During charging, the Na ions in the seawater were extracted and transported into the negative electrode compartment, followed by reduction to metallic Na at the negative electrode [Eq. (1)]:



On the positive electrode side, there were two major substances in seawater that could be oxidized at the electrode, namely, H<sub>2</sub>O molecules and Cl<sup>-</sup> ions, as shown in the half-cell reactions below [Eqs. (2) and (3)]:



Therefore, two possible overall reactions can be considered during the charging process [Eqs. (4) and (5)]:



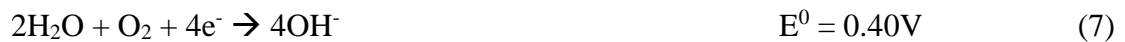
Evolution of gaseous phases occurs at the positive electrode in both chemical reactions, but the voltages for formation of O<sub>2</sub> and Cl<sub>2</sub> are slightly different (0.14 V).

Although O<sub>2</sub> evolution is thermodynamically preferred compared to Cl<sub>2</sub> evolution, the observed charge voltage of the salt water can be related to the reaction involved with both Cl<sub>2</sub> and O<sub>2</sub> gas evolution. More generally, the ratio of Cl<sub>2</sub> evolution is higher than that of O<sub>2</sub> evolution because of the higher overpotential of the O<sub>2</sub> evolution reaction when salt water [NaCl (aq)] undergoes an electrolytic process (Figure 2a).[7, 8] Our measured charge voltage (4.05 V) is slightly higher than the calculated standard voltage of O<sub>2</sub> evolution (3.94 V) and is similar to that of the Cl<sub>2</sub> evolution (4.07 V). This result indicates that the measured charge voltage is more related to Cl<sub>2</sub> evolution than to O<sub>2</sub> evolution, according to the literature.[7, 8] Indeed, the Na and Cl concentrations in seawater decreased after charge (see Table S1).

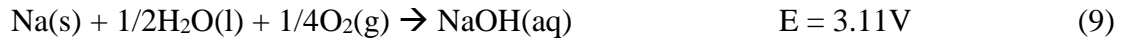
As shown in Figure 2b, the first discharge voltage of the prepared battery was ~2.9 V (vs. Na<sup>+</sup>/Na<sup>0</sup>), determined at a rate of 0.1 mA cm<sup>-2</sup>. During discharging of the battery, sodium ions generated from the Na metal at the negative electrode migrated into the seawater through the solid electrolyte. The following chemical reaction occurred at the negative electrode according to the half-cell reaction [Eq. (6)]:



At the positive electrode, two possible electrochemical reactions can be considered involving the reduction of water and dissolved oxygen [Eqs. (7) and (8)]:



Hence, two possible overall chemical reactions can be constructed, as shown below, when the battery is discharged [Eqs. (9) and (10)]:



There is a large difference in the cell voltages between Reactions (9) and (10), depending on whether dissolved  $\text{O}_2$  is involved in the positive electrode reaction or not. In our experiment, the observed discharge voltage of  $\sim 2.9$  V (vs.  $\text{Na}^+/\text{Na}^0$ ) was much higher than the 1.88 V (vs.  $\text{Na}^+/\text{Na}^0$ ) for the water-only reaction [Eq. (10)], but was similar to the 3.11 V (vs.  $\text{Na}^+/\text{Na}^0$ ) for Reaction (9), suggesting  $\text{O}_2$  involvement in the positive electrode reaction. To confirm the effect of dissolved  $\text{O}_2$  on the discharge voltage of the seawater,  $\text{O}_2$  was removed by bubbling  $\text{Ar}/\text{H}_2$  (95:5 wt%) gas into the seawater for 20 h before discharging the cell. A sharp voltage decrease to 1.8 V (vs.  $\text{Na}^+/\text{Na}^0$ ) from 2.9 V (vs.  $\text{Na}^+/\text{Na}^0$ ) was observed in the  $\text{Ar}/\text{H}_2$ -bubbled seawater cell under the same experimental conditions (Figure 2b). This experiment clearly demonstrates the contribution of dissolved  $\text{O}_2$  to the cell reaction with seawater. Similar results of voltage decreases in  $\text{O}_2$ -free water have been reported in the literature.[9, 10] The pH value was estimated to confirm  $\text{NaOH}$  generation after discharge, and the value increased from 7.8 to 9.2, according to the  $\text{NaOH}$  production. Based on the charge ( $\sim 4.05$  V vs.  $\text{Na}^+/\text{Na}^0$ ) and discharge voltages ( $\sim 2.9$  V vs.  $\text{Na}^+/\text{Na}^0$ ) in the first cycle, a voltage efficiency of about 73% was obtained at a current rate of  $0.1 \text{ mA cm}^{-2}$  (Figure 2c). Moreover, the charge–discharge voltage and voltage efficiency remained constant after

several cycles, without any change (Figure S3). The discharge voltage gradually decreased at higher current rates (Figure 2d) because of the increasing current.

In addition to using Na metal, we also tested Na-intercalated solid compounds as the negative electrode. Hard carbon is known to reversibly store sodium ions within its structure at a low voltage of  $<1.0$  V (vs.  $\text{Na}^+/\text{Na}^0$ ).<sup>[11, 12]</sup> Figure 3 a shows the voltage profiles during the first cycle with a half-cell of Na/carbon. A 28% irreversible capacity between charge and discharge was observed during the first cycle, which has been previously explained by the formation of a solid electrolyte interface (SEI) layer at the surface of the hard carbon.<sup>[13]</sup> After the irreversible first cycle, reversible voltage curves with slopes of 0.6–0.1 V (vs.  $\text{Na}^+/\text{Na}^0$ ) were observed, corresponding to the reversible storage of Na ions in the hard carbon structure during cycling.<sup>[14, 15]</sup> Based on the half-cell voltage curves for Na–carbon and Na–seawater (Figure 3 a), full-cell voltage curves for carbon–seawater can be predicted, which corresponded well to the measured slope voltage curves for the carbon–seawater full-cell (Figure 3b).

The carbon–seawater full cell had an average voltage of  $\sim 2.1$  V and a discharge capacity of  $\sim 115$  mAh  $\text{g}^{-1}$  at  $0.1$  mA  $\text{cm}^{-2}$ . The first cycle of the full-cell had a 69% Coulombic efficiency. The 31% irreversible capacity is due to the sodium ions initially harvested from the seawater being consumed to form a stable SEI layer on the surface of the hard carbon negative electrode. After formation of the SEI, the observed voltage slopes of 2.5–3.5 V corresponded to sodium ion intercalation into the hard carbon structure.<sup>[13]</sup> Furthermore, the discharge voltage was continually maintained during cycling due to continuous provision of  $\text{O}_2$  by the flowing seawater. The Coulombic efficiency of the full-cell clearly improved after the first cycle, and good capacity retention was obtained (Figures 3c

and 3d). The seawater battery system needs a solid electrolyte to be very stable in aqueous solution and the NASICON-type solid electrolyte showed good chemical stability throughout 40 cycles in contact with seawater (Figure S4). However, as its long-term stability in water is a concern,[16] further research is planned to evaluate its long-term stability in seawater and effects on electrochemical performance.

To investigate sodiation into a hard carbon anode, the hard carbon electrodes were carefully disassembled and washed using diethyl carbonate and then investigated by X-ray photoelectron spectroscopy (XPS) and scanning electron microscopy with energy dispersive X-ray spectroscopy (SEM-EDX). Figure 4a shows the high-resolution XPS core level spectra of Na 1 s. After the first charge, the intensity of Na 1 s significantly increases, indicating the Na ion uptake upon charge. Additionally the ex situ SEM-EDX analysis of carbon electrodes before and after the electrochemical sodiation reveals a very homogenous sodium distribution in the carbon layers (Figure 4b). These results demonstrate the possibility of replacing highly reactive metallic sodium by suitably designed high-capacity materials for such seawater batteries.

In summary, this study demonstrated the electrochemical mechanism of a novel rechargeable battery using seawater to provide both negative and positive source materials through charging and discharging of the cell. The seawater showed 4.05 V with Cl<sub>2</sub> evolution during charge and the discharge potential was 2.9 V with O<sub>2</sub> participation into the discharge reaction. Also, we found that sodium ions in flowing seawater reversibly intercalated into the hard carbon in the cell with good cycle performance. Studies of this novel battery are in an early stage and further design and performance improvements are under development. However, we expect it to have global application for stationary energy storage for wind and

solar energy farms, as seawater is an abundant, low-cost, and environmentally friendly material.

## Experimental Section

Na metal and seawater were purchased from Aldrich and used as the anode and cathode materials, respectively. The hard carbon negative electrode (3.2 mg) was fabricated from an 80:10:10 (wt%) mixture of hard carbon (MeadWestvaco Corp.), Super-P conductive carbon black (TIMCAL) as the current conductor, and polyvinylidene fluoride (Aldrich) as the binder. For the hybrid multi-layer electrolyte, 1 M NaClO<sub>4</sub> in ethylene carbonate/diethyl carbonate (1:1 volume ratio) was used as the non-aqueous liquid electrolyte and a NASICON-type Na<sub>3</sub>Zr<sub>2</sub>Si<sub>2</sub>PO<sub>12</sub> ceramic plate was used as the solid electrolyte. Na<sub>3</sub>Zr<sub>2</sub>Si<sub>2</sub>PO<sub>12</sub> was prepared by a solid-state reaction method. Powder Na<sub>3</sub>PO<sub>4</sub>·12H<sub>2</sub>O, SiO<sub>2</sub> and ZrO<sub>2</sub> were mixed and then calcined at 400 and 1100°C. After being mixed and calcined again, the powder was pressed into a pellet, which was sintered at 1230°C. The ion concentration of the seawater was determined by using inductively coupled plasma spectrometry (ICP, Atomscan 25, Optima 4300DV). Impedance spectroscopy experiments were carried out using a Solartron 1470E. For the impedance measurements, a Pt/NASICON/Pt cell was made by Pt sputtering. Carbon paper (Fuel Cell Store, Inc.) was placed in the seawater positive electrode as a current collector. The assembled cell was exposed to seawater and connected to a testing station. A battery cell tester (WBCS3000; Wonatech) was used to conduct charge and discharge tests at various current densities.

## Acknowledgements

This work was supported by the Creativity and Innovation Project Fund (1,140009,01) of Ulsan National Institute of Science and Technology (UNIST) and the Basic Science Research Program through the National Research Foundation of Korea (NRF) funded by the Ministry of Education (NRF-2014R1A1A2A16053515). A part of this work was also supported by the C-ITRC (Convergence Information Technology Research Center) support program (NIPA-2013-H0301-13-1009) supervised by the NIPA (National IT Industry Promotion Agency) through the Ministry of Science, ICT and Future Planning, Korea. Funding for the Argonne National Laboratory is from the Department of Energy (Contract DE-AC02-06CH11357) and is gratefully acknowledged.

## References

- [1] R. Black, S. H. Oh, J. H. Lee, T. Yim, B. Adams, L. F. Nazar, *J. Am. Chem. Soc.* **2012**, *134*, 2902 – 2905.
- [2] Y. Wang, Y. Wang, H. Zhou, *ChemSusChem* **2011**, *4*, 1087 –1090.
- [3] B. L. Ellis, L. F. Nazar, *Current Opinion in Solid State and Mater. Sci.* **2012**, *16*, 168–177.
- [4] Y. X. Yin, S. Xin, Y. G. Guo, L. J. Wan, *Angew. Chem. Int. Ed.* **2013**, *52*, 13186 –13200; *Angew. Chem.* 2013, *125*, 13426 –13441.
- [5] J. K. Kim, F. Mueller, H. Kim, J. S. Park, D. H. Lim, G. T. Kim, D. Bresser, S. Passerini, Y. Kim, *NPG Asia Mater.* **2014**, DOI: 10.1038/am.2014.106.

- [6] E. Brown, Butterworth-Heinemann (an imprint of Elsevier), *Seawater: Its Composition, Properties and Behaviour*, ISBN 978 –0 – 7506– 3715 –2, **1995**, Page: 29.
- [7] H. K. Abdel-Aal, S. M. Sultan, I. A. Hussein, *Int. J. Hydrogen Energy* **1993**, *18*, 545– 551.
- [8] H. K. Abdel-Aal, K. M. Zohdy, M. A. Kareem, *Open Fuel Cells J.* **2010**, *3*, 1–7.
- [9] K. Hayashi, K. Shima, F. Sugiyama, *J. Electrochem. Soc.* **2013**, *160*, A1467 –A1472.
- [10] H. He, W. Niu, N. M. Asl, J. Salim, R. Chen, Y. Kim, *Electrochim. Acta* **2012**, *67*, 87–94.
- [11] D. A. Stevens, J. R. Dahn, *J. Electrochem. Soc.* **2001**, *148*, A803–A811.
- [12] Y. Li, S. Xu, X. Wu, J. Yu, Y. Wang, Y. Hu, H. Li, L. Chen, X. Huang, *J. Mater. Chem. A* **2015**, DOI: 10.1039/c4ta05451b.4.
- [13] A. Ponrouch, A. R. Goni, M. Rosa Palacin, *Electrochem. Commun.* **2013**, *27*, 85– 88.
- [14] S. Komaba, W. Murata, T. Ishikawa, N. Yabuuchi, T. Ozeki, T. Nakayama, A. Ogata, K. Gotoh, K. Fujiware, *Adv. Funct. Mater.* **2011**, *21*, 3859 –3867.
- [15] X. Xia, M. Obrovac, J. R. Dahn, *Electrochem. Solid-State Lett.* **2011**, *14*, A130– A133.
- [16] R. O. Fuentes, F. Figueiredo, F. M. B. Marques, J. I. Franco, *Solid State Ionics* **2001**, *139*, 309– 314.

## Figures captions

**Figure 1.** a) Components of seawater. Schematic diagram of the cell at the b) charging and c) discharging states.

**Figure 2.** a) Charge voltage curves for the cell with seawater and 0.1 M NaCl solution and b) discharge voltage curves for the cell with seawater and Ar/H<sub>2</sub>-bubbled seawater measured at 0.1 mA cm<sup>-2</sup>. c) Discharge and charge voltage curves for the first cycle of the Na/seawater half-cell. d) Discharge voltage curves for the Na/seawater half-cell at different currents.

**Figure 3.** a) Initial discharge and charge voltage curves for the half-cells with Na/seawater and Na/hard carbon. b) Initial charge–discharge curve, c) cycled charge–discharge curves, and d) cycle performance and Coulombic efficiency of the hard carbon/seawater battery (0.1 mA cm<sup>-2</sup> at RT).

**Figure 4.** Ex situ a) XPS and b) SEM-EDX images of the hard carbon anode before and after charge, mapping the elemental distribution of C and Na.

Figure 1.

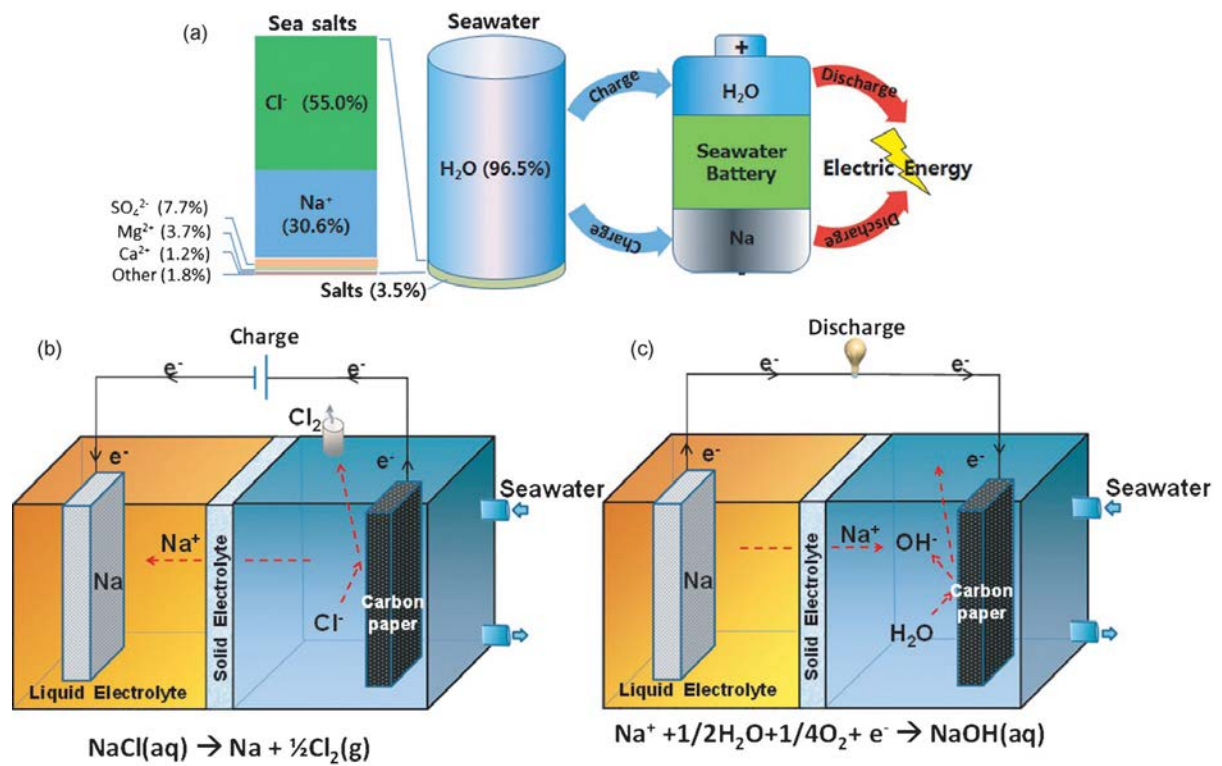


**Figure 2.**

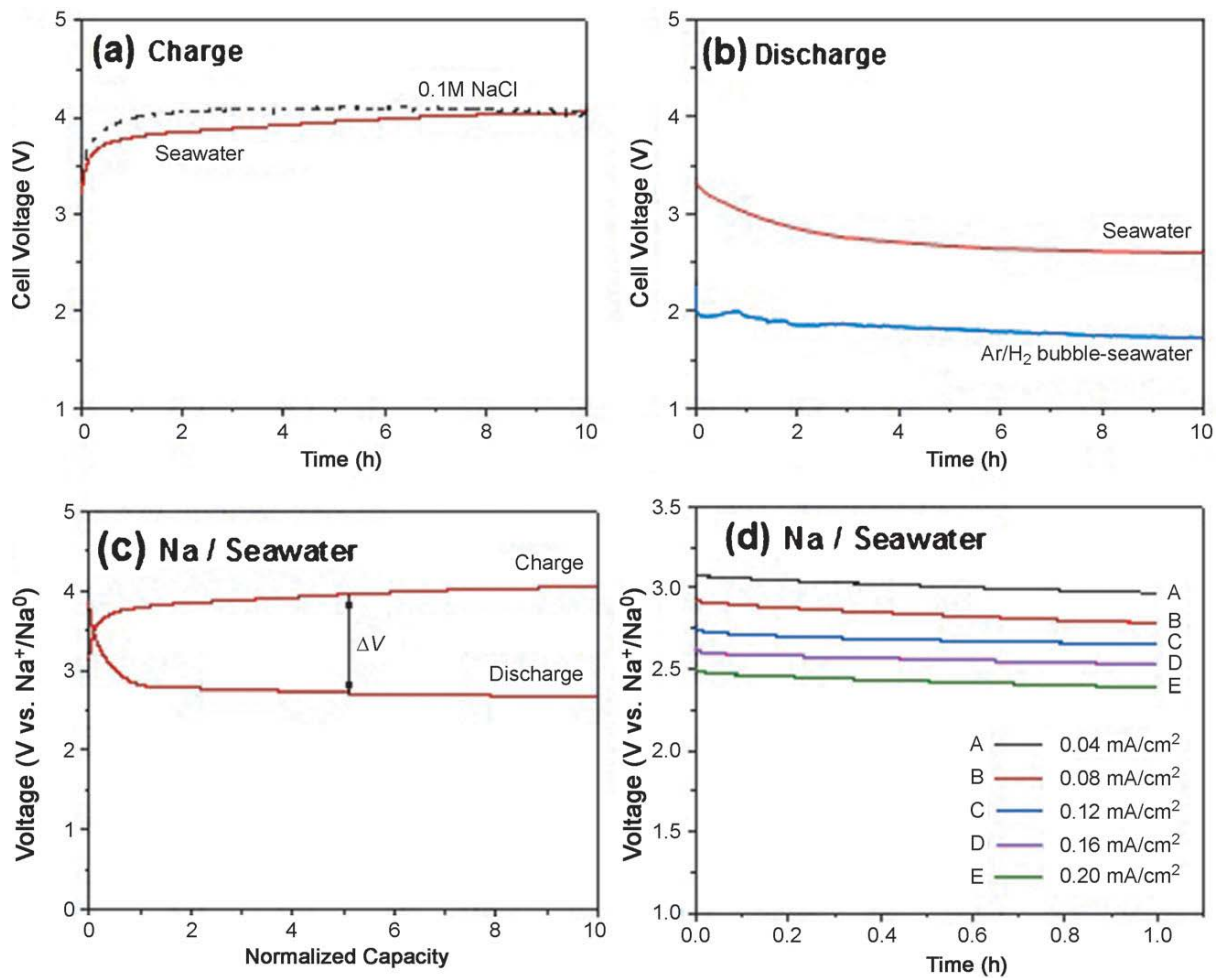


Figure 3.

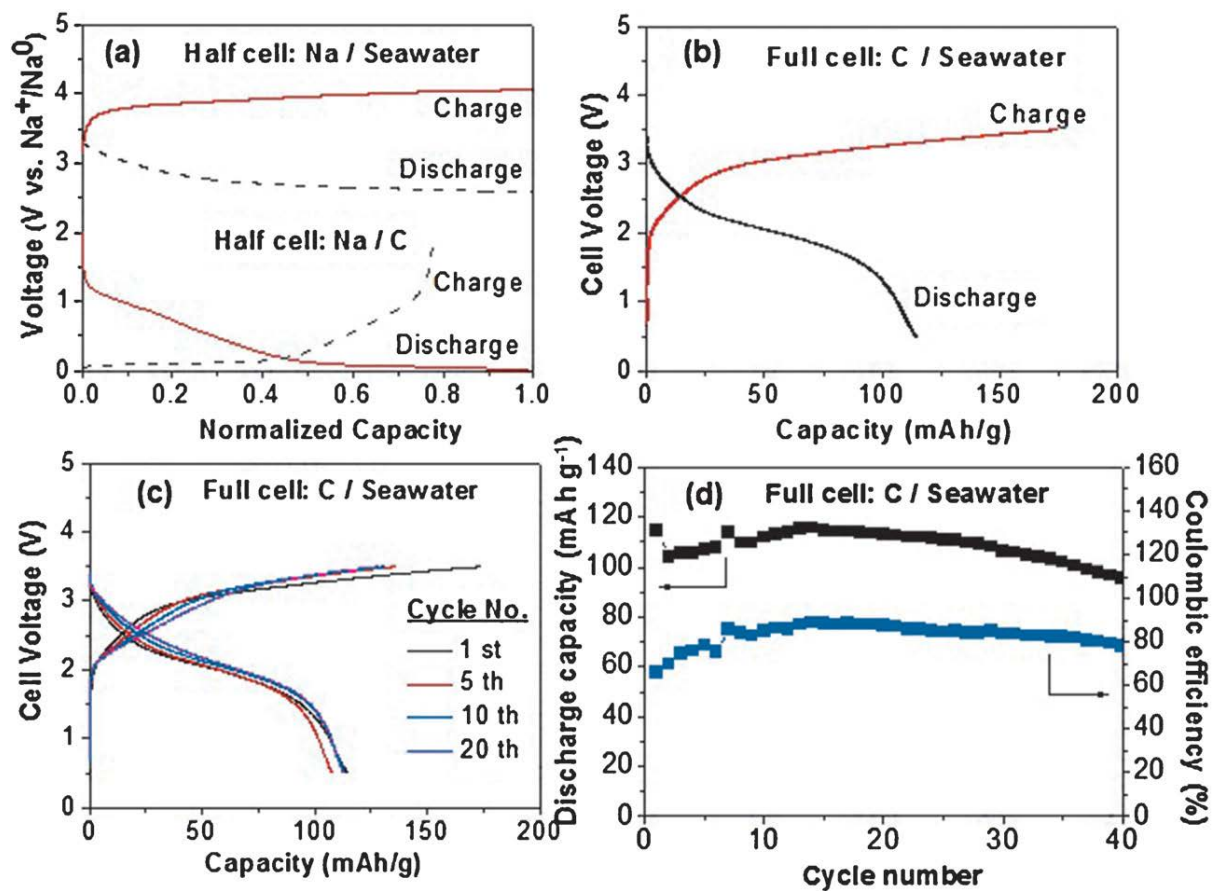


Figure 4.

